Nonlinear Robust Control to Maximize Energy Capture in a Variable Speed Wind Turbine

E. Iyasere[†], M. Salah, Ph.D. [‡], D. Dawson, Ph.D. [†], and J. Wagner, Ph.D., P.E. [†]
[†]College of Engineering and Science, Clemson University, Clemson, SC 29634
‡ Department of Mechatronics Engineering, the Hashemite University, Zarqa, Jordan

Abstract—**The emergence of wind turbine systems for electric power generation can help satisfy the growing global demand. To maximize wind energy captured in variable speed wind turbines at low to medium wind speeds, a robust control strategy is presented. The proposed strategy simultaneously controls the blade pitch and tip speed ratio, via the rotor angular speed, to an optimum point at which the efficiency constant (or power coefficient) is maximum. The control method allows for aerodynamic rotor power maximization without the restrictions of exact wind turbine model knowledge. A series of numerical results show that the wind turbine can be controlled to achieve maximum energy capture.**

I. Introduction

Wind energy has evolved into an attractive energy source for electric utilities, although it is currently responsible for only one percent of the global electrical power output. The structure of wind turbines, as well as the fact that the wind energy rate is uncontrollable, compounds the problem of regulating the power capture of the wind turbine. This problem has been alleviated by the construction of variable speed wind turbines, which are designed to regulate the power captured over a range of wind speeds. The efficiency of power regulation, is however dependent on the selected control method.

Windmill control methods include classical techniques [1], [2], [3], which utilize a linearized wind turbine system model and a single measured wind turbine output for control. In [2], a PID controller compensates for wind speed fluctuations by changing the pitch angle to keep the rotor speed constant. The controller is improved by selecting gain values based on minimization of rotor speed error and the actuator duty cycle. Another common control method is full state feedback [4], [5], [6], [7], which is sensitive to errors in modeling and measurements. Liebst [4] uses individual blade pitch linear quadratic Gaussian (LQG) optimal control to reduce the loads on a wind turbine due to environmental factors such as shear and gravity. The dynamics of the wind turbine blade flap, lag and pitch are modeled. Knudsen et al. [5] compare PI and H_∞ controllers for regulating the pitch of a 400kW wind turbine. The H_∞ controller accounts better for turbine model uncertainties as well as error in measuring the wind speed, thus reducing pitch activity. Disturbance accommodating control can account for measurement disturbances by augmenting a state-estimator based controller to recreate disturbance states using an assumed waveform model [8]. These new states reduce disturbance effects. Wright and Balas [8] describe the design of a state space control algorithm for the regulation of the rotor speed of a two bladed wind turbine in full-load operation using a simple five degree-of-freedom linear model. The authors demonstrate that the pole placement technique can stabilize the modeled turbine while state estimators reduce the number of required measurements. The wind speed fluctuations are reduced using disturbance accommodating control.

Fuzzy logic control [9], [10], [11] and neural networks [12] have been investigated to reduce the uncertainties faced by classical control methods. Prats et al. [10] present a fuzzy logic application for enhanced energy capture in a variable speed, variable pitch wind turbine. A dynamic model was developed using torque and blade pitch fuzzy control and produced better results than linear control. Zhang et al. [11] compared PID and fuzzy logic control in the control of the rotation of the wind wheel and reverse moment of the generator in a variable speed wind turbine and concluded that fuzzy logic control produce a smoother output with less susceptibility to disturbances. Adaptive control schemes [13], [14], [15], [16] have been developed to eliminate some of the problems faced in wind turbine control, such as unknown and time varying model parameters in the wind turbine model. Song et al. [14] used a model reference adaptive control scheme to force a wind turbine with a known power efficiency function, to track a desired rotor speed that maximizes the energy captured by controlling the excitation winding voltage of the generator. Johnson et al. [15] developed an adaptive control algorithm for controlling the generator torque on a fixed pitch variable speed wind turbine. This approach maximized the energy capture in low to medium wind speeds without knowledge of the optimal tip speed ratio.

In this study, a control strategy is developed to regulate the blade pitch angle and rotor speed of a variable speed wind turbine system. The control objective is to maximize the energy captured by the wind turbine in low to medium wind speeds by tracking a desired pitch angle and rotor speed, with the wind turbine system nonlinearities structurally uncertain. Additionally, the maximization of the energy captured is achieved without the knowledge of the relationship that governs the power capture efficiency of the wind turbine. Instead, an optimization algorithm is developed to seek the unknown optimal blade pitch angle and rotor speed that maximize the energy captured (via

Preprint submitted to 2008 American Control Conference.
Received September 17, 2007.

the aerodynamic rotor power) while ensuring that the resulting trajectories are sufficiently differentiable. The disadvantage of not explicitly knowing the optimal pitch angle and rotor speed *a priori* is countered by the fact that the optimal rotor speed, and likewise, the optimal pitch angle, will change as the wind speed changes, which can be accounted for by the optimization algorithm. A robust controller is used and proven to yield a globally uniformly ultimately bounded (GUUB) stable closed loop system through Lyapunov-based analysis.

The paper is organized as follows. In Section II, a wind turbine dynamic model will be presented. In Section III, a robust tracking controller is introduced along with the error system dynamics. The stability analysis is presented in Section IV. In Section V, the system nonlinearities have been estimated. The reference trajectory generation is discussed in Section VI, followed by numerical simulation results in Section VII. Concluding remarks are presented in Section VIII.

II. Dynamic Model Development

The selected wind turbine model consists of two subsystems: pitch (wind turbine blades and pitch actuator) and drive train (high-speed shaft, gearbox, low-speed shaft and generator). The aerodynamic rotor power is dependent on the available wind power and the power coefficient. The power coefficient is a function of two variables: the tip-speed ratio (TSR) and the blade pitch angle. The rotor power of the wind turbine, $P_{\text{aero}}(t) \in \mathbb{R}$, can be defined as

$$P_{\text{aero}} = \frac{1}{2} C_p(\lambda, \beta) \rho A v^3 \tag{1}$$

where $\rho \in \mathbb{R}$ is the air density, $A \in \mathbb{R}$ is the rotor swept area, $v(t) \in \mathbb{R}$ is the wind speed, $C_p(\cdot) \in \mathbb{R}$ denotes the power coefficient of the wind turbine, which is assumed to be unknown, $\lambda(t) \in \mathbb{R}$ is the tip-speed ratio, and $\beta(t) \in \mathbb{R}$ represents the blade pitch angle. The tip-speed ratio, $\lambda(t)$, is defined as

$$\lambda = \frac{\omega R}{v} \tag{2}$$

where $\omega(t) \in \mathbb{R}$ is the rotor speed and R is the rotor radius. From (1) and (2), it is clear that there exists an optimal rotor speed ω^*, and blade pitch angle β^*, for a particular wind speed at which the power capture efficiency is maximum, represented by $C_p^{\max}$, where $C_p^{\max} = C_p(\lambda^*, \beta^*)$.

The rotor power, $P_{\text{aero}}(t)$, can also be written as

$$P_{\text{aero}} = \tau_{\text{aero}} \omega \tag{3}$$

where $\tau_{\text{aero}}(t) \in \mathbb{R}$ is the aerodynamic torque applied to the rotor by the wind. An expression for $\tau_{\text{aero}}(t)$ can be derived from (1)-(3) as

$$\tau_{\text{aero}} = \frac{1}{2} \rho A R \frac{C_p(\lambda, \beta)}{\lambda} v^2 \tag{4}$$

In (1), it is assumed that $C_p(\cdot)$ is unknown, which implies that $\tau_{\text{aero}}(\cdot)$ is unmeasurable.

The wind turbine model structure can be written as

$$M\ddot{X} + f(\beta, \dot{X}, v) = \tau \tag{5}$$

where $X(t) \triangleq \left[\int \omega(t)\, dt \quad \beta(t)\right]^T \in \mathbb{R}^{2\times 1}$ are the state variables, $M = \begin{bmatrix} m_1 & 0 \\ 0 & m_2 \end{bmatrix} \in \mathbb{R}^{2\times 2}$ denotes the lumped inertia matrix, $f(\cdot) \triangleq \left[\tau_{\text{aero}}(\cdot) \quad N(\cdot)\right]^T \in \mathbb{R}^{2\times 1}$ represents the system nonlinearities, $N(\cdot) \in \mathbb{R}$ designates the pitch subsystem nonlinearities, and $\tau(t) \in \mathbb{R}^{2\times 1}$ is the control input torque.

To facilitate the control development process, the following model characteristics are assumed:

A.1: $v(t), \omega(t), \beta(t), \dot{\beta}(t)$ are measurable.

A.2: $v(t)$ is constant or slowly time varying.

A.3: R, A, ρ are known constants.

A.4: $v, \dot{v}, \ddot{v} \in \mathcal{L}_\infty$.

A.5: The function $f(\beta, \dot{X}, v)$ is unknown because $C_p(\cdot)$ is unknown.

A.6: $f(\beta, \dot{X}, v), \dot{f}(\beta, \dot{X}, \ddot{X}, \dot{v}), \ddot{f}(\beta, \dot{X}, \ddot{X}, \dddot{X}, \ddot{v}) \in \mathcal{L}_\infty$ if $\beta, \dot{X}, \ddot{X}, \dddot{X} \in \mathcal{L}_\infty$

A.7: M is a known symmetric, positive definite matrix.

Remark 1: $\left\| f(\beta, \dot{X}, v) \right\|$ can be upper bounded by a known function such that $\left\| f(\beta, \dot{X}, v) \right\| \le \rho_z(\beta, \dot{X})$.

III. Error System Development

The control objective is to maximize the aerodynamic rotor power of the wind turbine while tracking a developed desired rotor speed $\omega_d(t) \in \mathbb{R}$ and blade pitch angle $\beta_d(t) \in \mathbb{R}$ such that $\omega \to \omega_d$ and $\beta \to \beta_d$ as $t \to \infty$. To quantify this objective, measurement tracking errors denoted by $e_1(t), e_2(t) \in \mathbb{R}$ are defined as

$$e_1(t) \triangleq \omega_d(t) - \omega(t), \quad e_2(t) \triangleq \beta_d(t) - \beta(t) \tag{6}$$

Remark 2: $\omega_d(t), \beta_d(t)$ are planned online by utilizing a numerical-based two-dimensional optimization algorithm to maximize the rotor power $P_{\text{aero}}(t)$ such that

Preprint submitted to 2008 American Control Conference.
Received September 17, 2007.

$\beta_d \to \beta^*$, $\omega_d \to \omega^* \Rightarrow P_{\text{aero}} \to P_{\max} \triangleq \frac{1}{2} C_p{}^{\max} \rho A v^3$ where $\begin{bmatrix} \omega^* & \beta^* \end{bmatrix}^T$ is the set of constants resulting from the optimum seeking algorithm after convergence. $\omega_d(t)$ and $\beta_d(t)$ are designed such that $\omega_d(t), \dot{\omega}_d(t), \ddot{\omega}_d(t) \in \mathcal{L}_\infty$ and $\beta_d(t), \dot{\beta}_d(t), \ddot{\beta}_d(t), \dddot{\beta}_d(t) \in \mathcal{L}_\infty$.

The following filtered tracking error, denoted by $r_2(t) \in \mathbb{R}$, is defined to facilitate the subsequent controller design

$$r_2 \triangleq \dot{e}_2 + \mu e_2 \ , \ \dot{r}_2 = \ddot{e}_2 + \mu \dot{e}_2 \tag{7}$$

where $\mu \in \mathbb{R}$ is a positive constant.

Remark 3: Based on the definition of $r_2(t)$ given in (7), standard arguments can be used to prove that if $r_2(t) \in \mathcal{L}_\infty$, then $e_2(t), \dot{e}_2(t) \in \mathcal{L}_\infty$.

After forming a new set of states, $z(t) = \begin{bmatrix} e_1(t) & r_2(t) \end{bmatrix}^T$, taking its time derivative and pre-multiplying by M, the following expression can be obtained

$$M\dot{z} = M \begin{bmatrix} \dot{e}_1 \\ \ddot{e}_2 \end{bmatrix} + M \begin{bmatrix} 0 \\ \mu \dot{e}_2 \end{bmatrix} \tag{8}$$

$$M\dot{z} = M\ddot{X}_d - M\ddot{X} + M \begin{bmatrix} 0 \\ \mu \dot{e}_2 \end{bmatrix} \tag{9}$$

$$M\dot{z} = M\ddot{X}_d + f(\cdot) - \tau + M \begin{bmatrix} 0 \\ \mu \dot{e}_2 \end{bmatrix} \tag{10}$$

Based on the subsequent stability analysis in the next section and the structure of the open loop error system in (10), the control input $\tau(t)$ is designed as

$$\tau = M\ddot{X}_d + M \begin{bmatrix} 0 \\ \mu \dot{e}_2 \end{bmatrix} + \hat{f}_s(\cdot) + Kz + \frac{\rho_z^2(\cdot)}{\varepsilon} z \tag{11}$$

where $\hat{f}_s(\cdot) \triangleq \frac{1}{\tau_1 s + 1} \text{sat}\{\hat{f}(\cdot)\}$, $\hat{f}(\cdot)$ is an estimate of $f(\cdot)$, $K \in \mathbb{R}^+$ is a control gain and $\varepsilon \in \mathbb{R}^+$ is a small constant.

Remark 4: $\hat{f}_s(\cdot), \dot{\hat{f}}_s(\cdot) \in \mathcal{L}_\infty$ since $\text{sat}\{\cdot\} \in \mathcal{L}_\infty$ and $\frac{1}{\tau_1 s + 1}$ is a proper bounded filter, where $\tau_1 \in \mathbb{R}^+$ is a small constant. Thus, it may be assumed that $\left\| \hat{f}_s(\cdot) \right\| \le \rho_N$, where $\rho_N \in \mathbb{R}^+$.

Substituting the control torque from (11) into the open-loop dynamics of (10), results in the following closed-loop error system

$$M\dot{z} = f(\cdot) - \hat{f}_s(\cdot) - Kz - \frac{\rho_z^2(\cdot)}{\varepsilon} z \tag{12}$$

IV. Stability analysis

Theorem 1: Given the closed loop system of (12), all signals are bounded and the tracking error signals given in (6) are globally uniformly ultimately bounded (GUUB) in the sense that

$$\lim_{t \to \infty} \left| e_1(t) \right|, \left| e_2(t) \right| \le \bar{\varepsilon}_o \tag{13}$$

where $\bar{\varepsilon}_o$ is a small constant.

Proof: A non-negative function, denoted by $V(t) \in \mathbb{R}$, is defined as

$$V = \frac{1}{2} z^T M z \tag{14}$$

Since M is positive definite symmetric, then (14) can be lower and upper bounded by the inequality

$$\lambda_{\min} \|z\|^2 \le V(z) \le \lambda_{\max} \|z\|^2 \tag{15}$$

where $\lambda_{\min}$ and $\lambda_{\max}$ are the minimum and maximum eigenvalues of M, respectively.

After taking the time derivative of (14), and substituting (12), the following expression is obtained

$$\dot{V} = z^T \left[f - \hat{f}_s - Kz - \frac{\rho_z^2}{\varepsilon} z \right] \tag{16}$$

$$\dot{V} = -Kz^T z - \frac{\rho_z^2}{\varepsilon} z^T z + z^T f - z^T \hat{f}_s \tag{17}$$

The expression $\dot{V}(t)$ can be upper bound as

$$\dot{V} \le -K \|z\|^2 - \frac{\rho_z^2 \|z\|^2}{\varepsilon} + \|z\| \rho_z + \|z\| \rho_N \tag{18}$$

if $K = k_1 + k_2$ where $k_1, k_2 \in \mathbb{R}^+$, the nonlinear damping argument [17] may be applied to (18) to obtain

$$\dot{V} \le -k_1 \|z\|^2 + \varepsilon_o + \rho_z \|z\| \left[1 - \frac{\rho_z \|z\|}{\varepsilon} \right] \tag{19}$$

where $\varepsilon_o = \frac{\rho_N^2}{4k_2}$. From (19), if $\rho_z(\cdot) \left\| z(t) \right\| \ge \varepsilon$, then $\dot{V}(t) \le -k_1 \left\| z(t) \right\|^2 + \varepsilon_o$. Similarly, if $\rho_z(\cdot) \left\| z(t) \right\| < \varepsilon$, then $\dot{V}(t) \le -k_1 \left\| z(t) \right\|^2 + \varepsilon + \varepsilon_o$. In both cases, the following relationship exists

$$\dot{V} \le -\frac{k_1}{\lambda_{\max}} V + \varepsilon + \varepsilon_o \tag{20}$$

From (15) and (20), the term $\left\| z(t) \right\|$ can be upper bound as

Preprint submitted to 2008 American Control Conference.
Received September 17, 2007.

$$\|z(t)\| \le \sqrt{\beta_0 \exp(-\beta_1 t) + \beta_2 \left[1 - \exp(-\beta_1 t)\right]} \quad (21)$$

where $\beta_0 \triangleq \frac{\lambda_{\max}}{\lambda_{\min}} \|z(t_0)\|^2$, $\beta_1 \triangleq \frac{k_1}{\lambda_{\max}}$, and $\beta_2 \triangleq \frac{\lambda_{\max}}{k_1 \lambda_{\min}} (\varepsilon + \varepsilon_o)$.

From (21), it can be shown that $e_1(t), r_2(t) \in \mathcal{L}_\infty$. Using Remark 3, it can be implied that $e_2(t), \dot{e}_2(t) \in \mathcal{L}_\infty$. Similarly, (6) and Remark 2, allow for $\beta(t), \dot{X}(t) \in \mathcal{L}_\infty$. From A.6, it is apparent that $f(\cdot) \in \mathcal{L}_\infty$. It can be shown that $\tau(t) \in \mathcal{L}_\infty$ using (11). The application of standard signal chasing arguments permits the conclusion that all signals in the closed-loop system remain bounded. In particular, from (12), $\dot{z}(t), \dot{e}_1(t), \ddot{e}_2(t) \in \mathcal{L}_\infty$. The closed-loop system is thus globally uniformly ultimately bounded (GUUB) stable. Using A.6, it is clear that $\dot{f}(\cdot) \in \mathcal{L}_\infty$. After taking the time derivative of (11) and using Remark 4, it can be shown that $\dot{\tau}(t) \in \mathcal{L}_\infty$. After taking the time derivative of (5), it is apparent that $\ddot{X}(t) \in \mathcal{L}_\infty$. Finally it may be concluded that $\ddot{f}(\cdot) \in \mathcal{L}_\infty$ using A.6.

V. Estimation of System Nonlinearities

As previously stated, the objective of this paper is to maximize the aerodynamic rotor power of a variable speed wind turbine with structurally uncertain system nonlinearities. This model property requires that the system nonlinearities be estimated. The estimate of $f(\cdot)$, denoted by $\hat{f}(\cdot)$, is developed for two reasons:

I. $\hat{f}(\cdot)$ is used as a feed-forward term in the control design, through $\hat{f}_s(\cdot)$, to reduce the magnitude of the control input torque, $\tau(t)$.

II. From (3) and (4), $P_{\text{aero}}(t)$ is unmeasurable since $\tau_{\text{aero}}(t)$ is unmeasurable. By utilizing $\hat{f}(\cdot) = \left[\hat{\tau}_{\text{aero}}(\cdot) \quad \hat{N}(\cdot)\right]^T$, an estimate of the captured power, $\hat{P}_{\text{aero}}(t)$, can be realized where $\hat{P}_{\text{aero}}(t) = \hat{\tau}_{\text{aero}}(t)\omega(t)$.

In the robust control design, it has been proven that $f(\cdot), \dot{f}(\cdot), \ddot{f}(\cdot) \in \mathcal{L}_\infty$. Now consider the two systems

$$M\ddot{X} = \tau - f\left(\beta, \dot{X}, v\right), \quad M\ddot{\hat{X}} = \tau - \hat{f}(\cdot) \quad (22)$$

where $\hat{X}(t) \in \mathbb{R}^{2\times 1}$ denotes the estimate of the states, and $\hat{f}(\cdot)$ is the estimate of $f(\cdot)$. If $\hat{f}(\cdot)$ is known from the subsequently designed estimator, then $\dddot{\hat{X}} = M^{-1}\left(\dot{\tau} - \dot{\hat{f}}(\cdot)\right)$ where $\dot{\tau}(t)$ is measurable.

The objective of the estimator is to track the system nonlinearities $f(\cdot)$ such that $\hat{f}(\cdot) \to f(\cdot)$ as $t \to \infty$. To quantify this objective, the observation errors, $\ddot{\tilde{X}}(t), \dot{\tilde{f}}(t) \in \mathbb{R}^{2\times 1}$ are defined as

$$\ddot{\tilde{X}} = \ddot{\hat{X}} - \ddot{X}, \quad \dot{\tilde{f}} = \dot{\hat{f}} - \dot{f} \quad (23)$$

The filtered observation error, denoted by $r(t) \in \mathbb{R}^2$, is defined to facilitate the subsequent design and analysis

$$r = \dddot{\tilde{X}} + \Delta \ddot{\tilde{X}} \quad (24)$$

where $\Delta \in \mathbb{R}^+$ is a constant. After taking the time derivative of (24) and pre-multiplying by M, it may be shown that

$$M\dot{r} = M\ddot{\ddot{X}} + \Delta M\dddot{\tilde{X}} = -\ddot{\hat{f}} + \ddot{f} + \dot{\tilde{N}} - \dddot{\hat{X}} \quad (25)$$

where $\tilde{N}(\cdot) = \Delta M\dddot{\tilde{X}} + \ddot{\tilde{X}} \le \bar{\rho}_N \|\bar{z}\|$, $\bar{z}(t) = \left[\ddot{\tilde{X}}(t) \quad r(t)\right]^T$, and $\bar{\rho}_N \in \mathbb{R}^+$ is a constant. Based on the structure of (25) as well as the subsequent stability analysis, the following implementable continuous estimator law is proposed to achieve the stated estimator objectives

$$\ddot{\hat{f}} = (k + \Delta) r + \rho_0 \operatorname{sgn}\left(\dddot{\tilde{X}}\right) \quad (26)$$

where $k \in \mathbb{R}^+$ is a control gain.

Before presenting the stability analysis, the following lemma will be introduced and later invoked.

Lemma 1: Let the auxiliary function $L(t) \in \mathbb{R}$ be defined as

$$L \triangleq r^T\left(\dot{f} - \rho_0 \operatorname{sgn}\left(\ddot{\tilde{X}}\right)\right) \quad (27)$$

If the control gain ρ_0 is selected to satisfy the sufficient condition $\rho_0 > \left\|\dot{f}(\cdot)\right\| + \frac{\left\|\ddot{f}(\cdot)\right\|}{\Delta}$, then $\int_{t_0}^{t} L(\tau)\, d\tau \le \zeta_0$ where the positive constant $\zeta_0 \in \mathbb{R}$ is

$$\zeta_0 \triangleq \rho_o \left\|\ddot{\tilde{X}}(t_0)\right\|_1 + \ddot{\tilde{X}}^T(t_0)\dot{f}(t_0) \quad (28)$$

Proof: Refer to Appendix A.

Theorem 2: The estimator law of (26) ensures that all system signals are bounded and we obtain asymptotic tracking in the sense that $\tilde{f} \to 0$ as $t \to \infty$.

Proof: Define an auxiliary function $P(t) \in \mathbb{R}$ as follows

$$P = \zeta_o - \int L(\tau)\, d\tau \quad (29)$$

Preprint submitted to 2008 American Control Conference.
Received September 17, 2007.

where $\zeta_0, L(t)$ have been defined in Lemma 1. Based on the non-negativity of $P(t)$, a nonnegative function $V_1(t)$ may be defined as

$$V_1(t) = \frac{1}{2}\dot{\tilde{X}}^T\dot{\tilde{X}} + \frac{1}{2}r^T M r + P \tag{30}$$

After taking the time derivative of (30), utilizing the definitions in (24), (25), (27), (29), and rearranging terms, the following expression is obtained

$$\dot{V}_1 = -\Delta\dot{\tilde{X}}^T\dot{\tilde{X}} - r^T\dot{\tilde{f}} + r^T\tilde{N} + r^T\rho_0\,\mathrm{sgn}\left(\dot{\tilde{X}}\right) \tag{31}$$

After substituting (26) and performing simple algebraic manipulations, $\dot{V}_1(t)$ can be upper bounded by

$$\dot{V}_1 \le \Delta\|\bar{z}\|^2 + \left[\|r\|\bar{\rho}_N\|\bar{z}\| - k\|r\|^2\right] \tag{32}$$

where $\bar{z}(t)$ is a composite error vector previously defined in (25). Applying the nonlinear damping argument [17] to the bracketed term results in

$$\dot{V}_1 \le -\left[\Delta - \frac{\bar{\rho}_N^2}{4k}\right]\|\bar{z}\|^2 \tag{33}$$

From (33), it is possible to state that

$$\dot{V}_1 \le -\gamma\|\bar{z}\|^2 \ \text{ for } k > \frac{\bar{\rho}_N^2}{4\Delta} \tag{34}$$

where $\gamma \in \mathbb{R}$ is some positive constant of analysis. From (34) and the analysis in this section, $\bar{z}(t) \in \mathcal{L}_\infty$. From the definition of $\bar{z}(t)$, $\dot{\tilde{X}}(t), r(t) \in \mathcal{L}_\infty$. From (26), it is clear that $\dot{\tilde{f}}(\cdot) \in \mathcal{L}_\infty$. Using standard signal chasing arguments, it can be shown that the all the signals in the closed-loop system remain bounded. In particular, from (25), it may be concluded that $\dot{r}(t) \in \mathcal{L}_\infty$. Next, one can deduce that $\dot{\bar{z}}(t) \in \mathcal{L}_\infty$. After employing a corollary to Barbalat's Lemma [18], it can shown that $\lim_{t\to\infty}\|\bar{z}(t)\| = 0$. From the definition of $z(t)$, $\lim_{t\to\infty}\dot{\tilde{X}}(t), r(t) = 0$. From (24), it may be noted that $\lim_{t\to\infty}\ddot{\tilde{X}}(t) = 0$. From (22), the following relationship can be obtained.

$$M\ddot{\tilde{X}} = f - \hat{f} = -\tilde{f} \tag{35}$$

From (35), $\tilde{f}(t) \to 0$ as $t \to \infty$, which implies that $\hat{\tau}_{aero}(t) \to \tau_{\text{aero}}(t)$.

VI. Trajectory Generator

In Remark 2, it is assumed that a desired trajectory $\xi_d(t) = \left[\omega_d(t) \quad \beta_d(t)\right]^T$ can be generated such that $\xi_d(t), \dot{\xi}_d(t), \ddot{\xi}_d(t), \ddot{\beta}_d(t) \in \mathcal{L}_\infty$ and $\xi_d \to \xi^*$ where ξ^* is an unknown set of constants that maximizes the aerodynamic rotor power $P_{\text{aero}}(t)$. As stated previously, $P_{\text{aero}}(t)$ is unmeasurable. Thus, the estimated captured power $\hat{P}_{\text{aero}} = \hat{\tau}_{aero}\omega$ can be used instead. The optimum seeking algorithm used in this study is the Powell's Method. Powell's method only requires measurement of the output function $\hat{P}_{\text{aero}}(t)$ and an initial guess (not required to be close to the value of ξ^*). Powell's method can then find ξ^* by performing a series of one dimensional line maximizations (using Brent's Method) with convergence due to the non-trivial choice of search directions [19] (i.e., new directions are calculated using the extended parallel subspace property to avoid linear dependence).

To ensure that $\xi_d(t), \dot{\xi}_d(t), \ddot{\xi}_d(t), \ddot{\beta}_d(t) \in \mathcal{L}_\infty$, a filter based form of Powell's method is used, wherein at each iteration, $\xi_d(k)$ is passed through a set of third order stable and proper low pass filters to generated continuous bounded signals for $\xi_d,(t)\dot{\xi}_d(t), \ddot{\xi}_d(t), \ddot{\beta}_d(t)$. The filters shown in (36)-(39) are used in this study, where $\zeta_1, \zeta_2, \zeta_3, \zeta_4 \in \mathbb{R}^+$ are filter constants. The optimization algorithm waits until certain error thresholds are met before making the next guess (i.e., if $\|\xi_d(t) - \xi_d(k)\| \le \bar{e}_1$, $\left|\tilde{f}(\cdot)\right| \le \bar{e}_2$ and $\|\xi(t) - \xi_d(t)\| \le \bar{e}_3$ then $k = k+1$) where $e_1, e_2, e_3 \in \mathbb{R}^+$ are constants and $k = 1, 2, \ldots$

$$\xi_d(t) = \frac{\zeta_1}{s^3 + \zeta_2 s^2 + \zeta_3 s^3 + \zeta_4}\xi_d(k) \tag{36}$$

$$\dot{\xi}_d(t) = \frac{\zeta_1 s}{s^3 + \zeta_2 s^2 + \zeta_3 s^3 + \zeta_4}\xi_d(k) \tag{37}$$

$$\ddot{\xi}_d(t) = \frac{\zeta_1 s^2}{s^3 + \zeta_2 s^2 + \zeta_3 s^3 + \zeta_4}\xi_d(k) \tag{38}$$

$$\ddot{\beta}_d(t) = \frac{\zeta_1 s^3}{s^3 + \zeta_2 s^2 + \zeta_3 s^3 + \zeta_4}\beta_d(k) \tag{39}$$

VII. Simulation Results

A numerical simulation is presented in this section to illustrate the performance of the controller introduced in (11), and to demonstrate the numerical-based optimum seeking reference trajectory generator. The system model in (5) was assumed to have the following system nonlinearities

Preprint submitted to 2008 American Control Conference.
Received September 17, 2007.

$$f(\cdot)=\left[\frac{1}{2}\rho A\frac{C_p(\lambda,\beta)}{\omega}v^3 \quad c\beta\right]^T \qquad (40)$$

where c is the blade damping coefficient. The model parameters are listed in Appendix B. The pitch angle and rotor speed tracking errors $e_1(t), e_2(t)$, shown in Fig. 1, settle to a small neighborhood around zero. The power coefficient function $C_p(\lambda,\beta)$, illustrated in Fig. 2a., was obtained using blade-element momentum theory [20]. For this case, $C_p^{\max}=0.4405$ at $\left[\lambda^*=8 \quad \beta^*=2.4\right]$ which according to (2), corresponds to $\left[\omega^*=8 \quad \beta^*=2.4\right]$. The numerical-based optimum seeking algorithm converged to $\left[\omega^*=8.004 \quad \beta^*=2.41\right]$ as shown in Figs. 2c and 2d. In Fig. 2b, the maximum simulated power coefficient was $C_p^{\max}=0.4404$. After analysis, the following three conclusions can be made. First, the results of the optimum seeking algorithm were within one percent of the nominal optimum blade pitch angle and rotor speed. Second, the tracking errors, $e_1(t), e_2(t)$, for both subsystems settle to a neighborhood of $\pm 5\times 10^{-3}$ around zero after 300 seconds. Finally, the control input $\tau(t)$ is bounded as shown in Fig. 3. Overall, the control strategy proposed in this study produced favorable results.

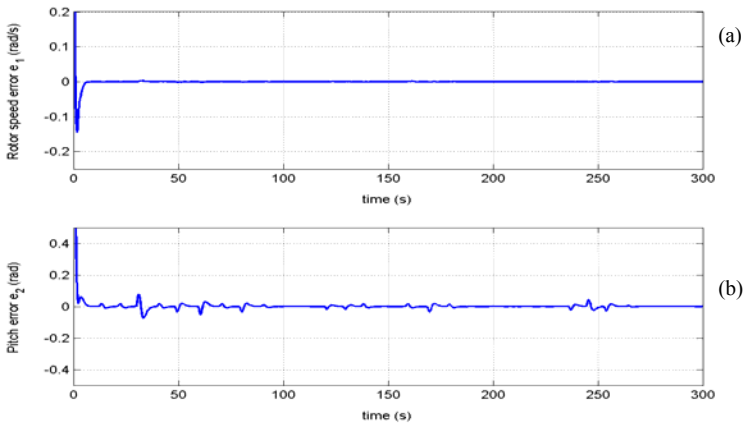

Fig. 1: Wind turbine tracking errors for (a) rotor speed $e_1(t)$, and (b) blade pitch angle $e_2(t)$.

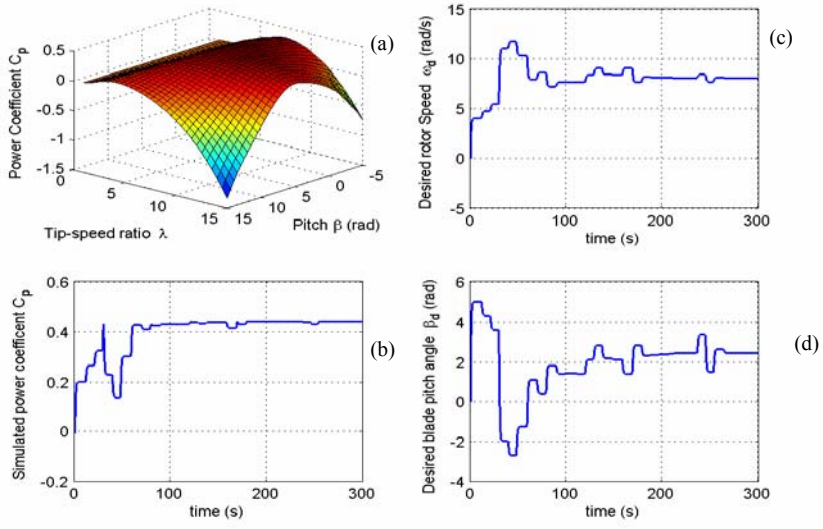

Fig. 2: (a) Power coefficient function C_p versus tip-speed ratio λ, and blade pitch angle β, for the simulated wind turbine, (b) maximum rotor power coefficient $C_p^{\max}(t)$ resulting from optimization algorithm, (c) desired rotor speed trajectory $\omega_d(t)$, and (d) desired blade pitch angle trajectory $\beta_d(t)$

Preprint submitted to 2008 American Control Conference.
Received September 17, 2007.

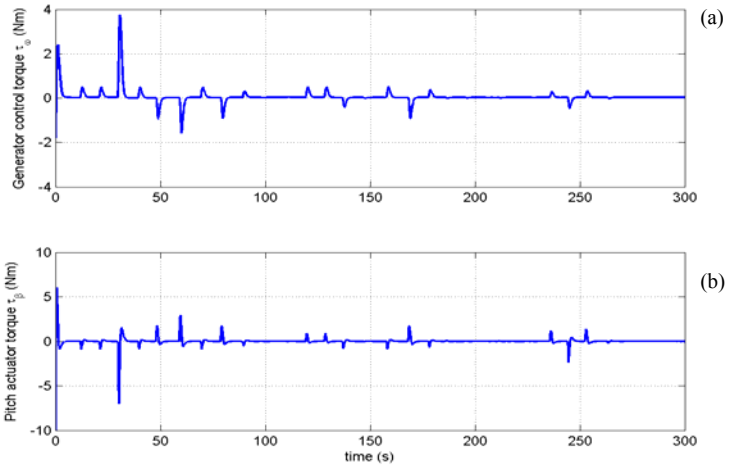

Fig.3: The simulated control torques for the (a) drive train subsystem, $\tau_\omega(t)$, and (b) pitch subsystem, $\tau_\beta(t)$

VIII. Conclusions

A nonlinear controller has been developed for a variable speed wind turbine system to optimize the energy captured by the wind turbine. A desired blade pitch angle and rotor speed trajectory generator is provided that seeks the unknown optimal set-point while ensuring the trajectory remains bounded and sufficiently differentiable. To track the desired trajectory, a robust controller is developed, which is proven to yield a globally uniformly ultimately bounded stable closed-loop system via Lyapunov-based analysis. Simulation results demonstrated the excellent performance of the robust controller and the numerical-based optimum seeking algorithm.

References

[1] M. Hand and M. Balas, "Non-linear and linear model based controller design for variable-speed wind turbines," presented at the 3rd ASME/JSME Joint Fluids Engineering Conf., San Francisco, CA, 1999.

[2] B. Malinga, J. Sneckenberger, and J. Feliachi, "Modeling and control of a wind turbine as a distributed resource," in *Proc. 35th Southeastern Symp. Syst. Theory*, Morgantown, WV, 2003, pp. 108-112.

[3] J. Svensson and E. Ulen, "The control system of WTS-3 instrumentation and testing," in *Proc. 4th Int. Symp. Wind Energy Systems*, Stockholm, Sweden, 1982, pp. 195-215.

[4] B. Liebst, "Pitch control system for large-scale wind turbines," *J. of Energy*, vol. 7, no. 2, pp.182-192, March 1983.

[5] T. Knudsen, P. Andersen, and S. Tiffner-Clausen, "Comparing PI and robust control pitch controllers on a 400KW wind turbine by full scale tests," Department of Control Engineering, Aalborg University, Aalborg, Denmark, Tech. Rep. R-97-4174, 1997.

[6] S. Mattson, ''Modeling and control of large horizontal axis wind power plants,'' Ph.D. Thesis, Lund Institute of Technology, Lund, Sweden, 1984.

[7] K. Stol and M. Balas, "Full-state feedback control of a variable-speed wind turbine: A comparison of periodic and constant Gains", *J. of Solar Energy Eng.*, vol. 123, no. 4, pp. 319-326, 2001.

[8] A. Wright and M. Balas, "Design of state-space-based control algorithms for wind turbine speed regulation," *J. Solar Energy Eng.,* vol. 125, no. 4, pp. 386-395, Nov. 2003.

[9] R. Chedid, S. Karaki, and C. El-Chamali, "Adaptive fuzzy control for wind-diesel weak power systems," *IEEE Trans. Energy Conversion*, vol. 15, no. 1, pp. 71-78, March 2000.

[10] M. Prats, J. Carrasco, E. Galvan, J. Sanchez, L.Franquelo and C. Batista, "Improving transition between power optimization and power limitation of variable speed, variable pitch wind turbines using fuzzy control techniques," *Proc. IECON 2000*, Nagoya, Japan, 2000, vol. 3, pp. 1497-1502,.

[11] X. Zhang, W. Wang and Y. Liu, "Fuzzy control of variable speed wind turbine", in *Proc. 6th World Congress on Intelligent Control and Automation*, pp. 3872-3876, Dalian, China, 2006.

[12] F. Kanellos and N. Hatziargyriou, "A new control scheme for variable speed wind turbines using neural networks," in *Proc. IEEE Power Eng. Soc. Trans. Distrib. Conf.*, New York, NY, 2002, pp. 360-365.

[13] J. Freeman and M. Balas "An investigation of variable speed horizontal-axis wind turbines using direct model-reference adaptive control" in *Proc. 18th ASME Wind Energy Symp.*, Reno, NV, 1999, pp. 66-76.

[14] Y. Song, B. Dhinakaran, and X. Bao, "Variable speed control of wind turbines using nonlinear and adaptive algorithms," *J. Wind Eng. Ind. Aerodyn.*, vol. 85, no. 3, pp. 293-308, Apr. 2000.

[15] K. Johnson, L. Fingersh, M. Balas, and L. Pao, "Methods for increasing region 2 power capture on a variable-speed wind turbine", *J. Solar Energy Eng.*, vol. 126, no. 4, pp. 1092-1100, 2004.

[16] K. Johnson, L. Pao, M. Balas, and L. Fingersh, "Control of variable-speed wind turbines: Standard and adaptive techniques for maximizing energy capture", *IEEE Control Syst. Mag.*, vol. 26, no. 3, pp. 70-81, June 2006.

[17] P. Kokotovic, "The joy of feedback: nonlinear and adaptive," *IEEE Control Syst. Mag.*, vol. 12, no. 3, pp. 7-17, June 1992.

[18] J. Slotine and W. Li, *Applied Nonlinear Control*, Englewood Cliffs, NJ: Prentice Hall, 1991.

[19] G. Reklaitis, A. Ravindran, and K. Ragsdell, *Engineering Optimization*, Hoboken, NJ: John Wiley & Sons, 1983, pp. 41-130.

Preprint submitted to 2008 American Control Conference.
Received September 17, 2007.

[20] NWTC Design Codes (WT_Perf by Marshall Buhl), http://wind.nrel.gov/designcodes/simulators/wtperf/, Aug. 1, 2007.

APPENDIX

A. Proof of Lemma 1

The proof for Lemma 1 used in Section V will now be presented. The equation (24) can be substituted into (27) and then integrated in time to obtain

$$\int_{t_0}^{t} L(\tau)\,d\tau = \int_{t_0}^{t} \Delta\dot{\tilde{X}}(\tau)^T \left(\dot{f}(\tau) - \rho_0 \operatorname{sgn}\left(\dot{\tilde{X}}(\tau)\right)\right) d\tau + \left[\int_{t_0}^{t} \frac{d\dot{\tilde{X}}^T(\tau)}{d\tau}\dot{f}(\tau)\,d\tau\right] - \rho_0 \int_{t_0}^{t} \ddot{\tilde{X}}^T(\tau)\operatorname{sgn}\left(\dot{\tilde{X}}\right) d\tau \tag{41}$$

The bracketed term in (41) may be integrated by parts so that the simplified expression becomes

$$\begin{aligned}\int_{t_0}^{t} L(\tau)\,d\tau = \int_{t_0}^{t} \Delta\dot{\tilde{X}}(\tau)^T \left(\dot{f}(\tau) - \frac{\ddot{f}(\tau)}{\Delta} - \rho_0 \operatorname{sgn}\left(\dot{\tilde{X}}(\tau)\right)\right) d\tau \\ + \dot{\tilde{X}}(t)\dot{f}(t) - \dot{\tilde{X}}(t_0)\dot{f}(t_0) - \rho_0 \left\|\dot{\tilde{X}}(t)\right\|_1 \\ + \rho_0 \left\|\dot{\tilde{X}}(t_0)\right\|_1\end{aligned} \tag{42}$$

An upper bound on the right hand side of (42) can be written as

$$\begin{aligned}\int_{t_0}^{t} L(\tau)\,d\tau = \int_{t_0}^{t} \Delta \left\|\dot{\tilde{X}}(\tau)\right\|_1 \left(\left\|\dot{f}(\tau)\right\| + \frac{\left\|\ddot{f}(\tau)\right\|}{\Delta} - \rho_0\right) d\tau \\ + \left\|\dot{\tilde{X}}(t)\right\|_1 \left(\left\|f(t)\right\| - \rho_0\right) + \rho_0 \left\|\dot{\tilde{X}}(t_0)\right\|_1 \\ - \dot{\tilde{X}}(t_0)^T f(t_0)\end{aligned} \tag{43}$$

From (43), if $\rho_0 > \left\|\dot{f}(\cdot)\right\| + \frac{\left\|\ddot{f}(\cdot)\right\|}{\Delta}$, then Lemma 1 holds.

B. Simulation parameters

Table I shows the values of the parameters used in the numerical simulation of Section VII.

TABLE I
SIMULATION PARAMETERS AND VALUES

Variables	Value	Units
m_1	1	kg.m^2
m_2	1	kg.m^2
R	1	m
v	1	m.s^2
A	1	m^2
c	0.5	kg.m^2/s
ρ	1	kg/m^3
ε	1	-
K	2.5	-
μ	2	-
k	1.5	-
Δ	1	-

C. Nomenclature list

TABLE II
NOMENCLATURE LIST

A	Rotor swept area (m^2)
c	Blade damping coefficient (kg.m^2/s)
C_p	Power coefficient
$C_{p_{max}}$	Maximum rotor power coefficient
e_1	Rotor speed tracking error (rad/s)
e_2	Blade pitch angle tracking error (rad)
$f(\cdot)$	System nonlinearities (N.m)
$\hat{f}(\cdot)$	Estimated system nonlinearities (N.m)
M	Lumped inertia matrix (kg.m^2)
$N(\cdot)$	Pitch subsystem nonlinearities (N.m)
$\hat{N}(\cdot)$	Estimated pitch subsystem nonlinearities (N.m)
P_{aero}	Rotor power (W)
P_{max}	Maximum rotor power (W)
R	Rotor radius (m)
t	Time (sec)
v	Wind speed (m.s^2)
X	State variables
β	Blade pitch angle (rad)
β_d	Desired blade pitch angle (rad)
β^*	Optimal blade pitch angle (rad)
λ	Tip-speed ratio (TSR)
λ^*	Optimal TSR
$\lambda_{\min}, \lambda_{\max}$	Eigenvalues of M
ρ	Air density (kg/m^3)
τ_{aero}	Aerodynamic torque (N.m)
$\hat{\tau}_{aero}$	Estimated aerodynamic torque (N.m)
τ	Control torque (N.m)
ω	Rotor angular speed (rad/s)
ω^*	Optimal rotor speed
ω_d	Desired rotor angular speed (rad/s)

Preprint submitted to 2008 American Control Conference.
Received September 17, 2007.